Angular correlations in the e^+e^- decay of excited states in ^{8}Be

A. C. Hayes,[1] J. Friar,[1] G. M. Hale,[1] and G. T. Garvey[1,2]
[1]*Los Alamos National Laboratory, Los Alamos, New Mexico 87545, USA*
[2]*Department of Physics, University of Washington, Seattle, Washington 98195, USA*

(Received 7 June 2021; revised 28 December 2021; accepted 24 January 2022; published 16 May 2022)

Motivated by the recent observation of anomalous electron-positron angular correlations in the decay of the 18.15-MeV 1^+ excited states in ^{8}Be, we reexamine in detail the standard model expectations for these angular correlations. The 18.15-MeV state is above particle threshold, and several multipoles can contribute to its e^+e^- decay. We present the general theoretical expressions for e^+e^- angular distributions for nuclear decay by $C0$, $C1$, $C2$, $M1$, $E1$, and $E2$ multipoles, and we examine their relative contribution to the e^+e^- decay of ^{8}Be at 18.15 MeV. We find that this resonance is dominated by $M1$ and $E1$ decay, and that the ratio of $M1$ to $E1$ strength is a strong function of energy. This is in contrast to the original analysis of the e^+e^- angular distributions, where the $M1/E1$ ratio was assumed to be a constant over the energy region $E_p = 0.8$–1.2 MeV. We find that the existence of a "bump" in the measured angular distribution is strongly dependent on the assumed $M1/E1$ ratio, with the present analysis finding the measured large-angle contributions to the e^+e^- angular distribution to be lower than expectation. Thus, in the current analysis we find no evidence for axion decay in the 18.15-MeV resonance region of ^{8}Be.

DOI: 10.1103/PhysRevC.105.055502

I. INTRODUCTION

Recently, an anomaly has been observed [1] in the electron-positron pair decay of an $M1$ resonance in ^{8}Be. In particular, the observed angle between the emitted e^+ and e^- pair in the transition of the 18.15-MeV 1^+ resonance to the ground state of ^{8}Be deviated significantly from expectation, and shows a so-called bump or shoulder at angles greater than 110°. The experiment [1] populated resonances in ^{8}Be via the ^{7}Li $+p$ reaction and observed their decay by detecting e^+e^- pairs. Many multipoles can contribute to the observed pair decay with the particular linear combination being determined by the nuclear structure of the ^{8}Be continuum at each incident proton energy. Interference between multipoles can also occur. In this experiment, the e^+e^- detectors were set at 90° to the incident beam, which tends to minimize the effects of interference. For this reason, we believe the interference effects are small but we could not reliably estimate them without a simulation of the experimental setup and detector responses. If the detectors' resolution and efficiency are symmetric about 90° to the incident beam, the only effect that can create interference between different multipoles is the small asymmetry due to the velocity of the decaying ^{8}Be.

The present work focuses on the expectations for the angular distributions for the decay of the 1^+ resonances in ^{8}Be by e^+e^- decay from standard electromagnetism applied to nuclear physics. Earlier work by Zhang and Miller [2] also examined some of the nuclear physics expectations for these decays, including anisotropy and multipole interference effects. These authors further examined [3] the predictions for e^+e^- decays from photonic vector boson production. They concluded that they could not find a reasonable physical explanation for the measured [1] angular distributions. In the present work, we concentrate on the $M1$ to $E1$ ratio involved in these decays, using the measured ^{7}Li(p,γ) data to constrain this ratio. The approach is motivated by the fact that the nuclear physics of the $M1$ and $E1$ decays in the (p,γ) reaction is identical to that for the (p,e^+e^-) reaction, so that the energy-dependent $M1/E1$ ratios have to be identical for the two reactions. However, the kinematics for the virtual photon in the (p,e^+e^-) reaction differs from the kinematics for the real photon in the (p,γ) reaction, and we derive the distribution for the angle between the emitted e^+ and e^- emitted in the (p,e^+e^-) reaction from first principles. These angular distributions were derived previously by Rose [4] long ago. His results are correct (which we have verified), but his approach is difficult to follow, given the techniques used at that time. Moreover the results are cast in a particularly obscure form. The potential importance of the use of the (p,e^+e^-) reaction for axion searches, and the fact that a textbook derivation is not available, suggests that a new derivation using modern techniques and notation would be valuable.

II. FORMALISM FOR e^+e^- ANGULAR DISTRIBUTIONS

The e^+e^- process is a mechanism in which the nucleus emits a virtual photon which then decays to an e^+e^- pair. The process is exactly analogous to electron scattering, but with the incident electron of momentum p in the scattering process being substituted by the outgoing positron in the decay: The momentum of the positron becomes $\bar{p} = -p \equiv (\bar{E}, \bar{\mathbf{p}})$. If the 3-momentum of the emitted electron is $\mathbf{p}'$, the momentum

transfer is $q = -(\bar{p} + p')$ and $\mathbf{q} = -(\bar{\mathbf{p}} + \mathbf{p}')$. Thus, our convention is that $\mathbf{q}$ is directed into the nucleus. We also ignore Coulomb effects and treat the lepton wave functions as plane waves. We believe this to be a reasonable assumption because Coulomb effects are important at a significant level only in the case of low-energy and low-momentum transfer, when the lepton can spend a long time in the Coulomb field. For the ^{7}Li(p, e^+e^-) of interest in the present work, the energy and momentum transfers are not particularly low. We note that Rose [4] also ignored Coulomb effects is his treatment of e^+e^- radiative decay.

For energies that allow a nonrelativistic treatment of the nuclear physics, the e^+e^- decay by a single nuclear state is determined by the momentum- and nuclear-structure-dependent electromagnetic charge and current operators, whose separate contributions are described throughout this work by the nuclear charge and nuclear current structure functions $T^{00}(\mathbf{q})$ and $T^{\perp\perp}(\mathbf{q})$, respectively.

The first function, $T^{00}(\mathbf{q})$, is defined in terms of matrix elements of the nuclear charge operator as

$$T^{00}(\mathbf{q}) = \overline{\sum_{f,i}} |\langle J_f M_f \mid \rho(\mathbf{q}) \mid J_i M_i \rangle|^2, \tag{1}$$

where $\rho(\mathbf{q}) = \int d^3x\ \rho(\mathbf{x})\ e^{i\mathbf{q}\cdot\mathbf{x}}$ and $\rho(\mathbf{x})$ is the nuclear charge operator. The overscore on the summation sign in Eq. (1) means average over initial nuclear spin projections (M_i) and sum over final ones (M_f). We assume that there is no initial-state or target polarization involved.

When expanded in spherical harmonics, the charge operator T^{00} becomes

$$T^{00} = \frac{4\pi}{2J_i + 1} \sum_{l \geqslant 0} |\langle J_f \mid\mid C_l \mid\mid J_i \rangle|^2, \tag{2}$$

where the normal-parity $[(-1)^l]$ charge multipole operator is given by

$$C_{lM} = \int d^3x\ \rho(\mathbf{x}) j_l(qx) Y_{lM}(\hat{x}). \tag{3}$$

We follow a standard, but not universal, notation that denotes charge multipoles by CJ, (i.e., $C0, C1, C2$, etc.). Thus the charge multipoles are distinguished from current multipoles, both electric ($E1, E2$, etc.) and magnetic ($M1, M2$, etc.). In the limit of small q, current conservation mandates that the EJ are proportional to CJ (for $J \geqslant 1$), which is known as Siegert's theorem. Only $C0$ is unique in origin via the charge operator and does not contribute to real photon decay.

The second structure function, $\mathrm{T}^{\perp\perp}(\mathbf{q})$, is defined in analogy to Eq. (1), with the charge operators replaced by current operators with space components m and n: $J^m(\mathbf{q}) = \int d^3x\ J^m(\mathbf{x})\ e^{i\mathbf{q}\cdot\mathbf{x}}$, etc. Only the summed components of the nuclear currents that are perpendicular to the vector $\mathbf{q}$ contribute: $\mathrm{T}^{\perp\perp}(\mathbf{q}) = \mathrm{T}^{mn}(\mathbf{q})\ (\delta^{mn} - \hat{\mathbf{q}}^m\hat{\mathbf{q}}^n)$. Expanding the exponential in terms of spherical harmonics and using the 1^- character of the current (as indicated by the subscript 1 on J, i.e., J_1) lead to the requisite operators,

$$O^l_{JM} = \int d^3x\ j_l(qx)(J_1(\mathbf{x}) \otimes Y_l(\hat{x}))_{JM}. \tag{4}$$

TABLE I. The relations among $\bar{E}, E', \bar{p}, p', q^2, \mathbf{q}^2, Q, x, y$, and r_Q, where $r_Q \equiv \frac{2m_e}{Q}$.

Variable definitions	
$\bar{E} = \frac{Q}{2}(1+y)$	$E' = \frac{Q}{2}(1-y)$
$\bar{p} = \frac{Q}{2}\sqrt{(1+y)^2 - r_Q^2}$	$p' = \frac{Q}{2}\sqrt{(1-y)^2 - r_Q^2}$
$q^2 = -2(m_e^2 + \bar{E}E' - \bar{p}p'x)$	$\mathbf{q}^2 = \bar{p}^2 + p'^2 + 2\bar{p}p'x$

Only $J \geqslant 1$ contributes to $T^{\perp\perp}$ and we find

$$T^{\perp\perp} = \frac{4\pi}{2J_i + 1} \sum_{J \geqslant 1} \left(|\langle J_f \mid\mid O^{J-1}_J \mid\mid J_i \rangle|^2 \left(\frac{J+1}{2J+1} \right) + |\langle J_f \mid\mid O^J_J \mid\mid J_i \rangle|^2 \right). \tag{5}$$

The first set of matrix elements in Eq. (5) produces electric (EJ) transitions and the second produces magnetic (MJ) transitions, with $J \geqslant 1$ in both cases.

If we denote the e^+e^- decay rate by $\omega_{e^+e^-}$, we find that the general form of the e^+e^- angular distribution is given directly in the Coulomb gauge for the virtual photon by

$$\frac{d^2\omega_{e^+e^-}}{dxdy} = \frac{2\alpha^2 \bar{p}\, p'\, Q}{\pi q^4} \left\{ T^{00}(\mathbf{q}) \frac{q^4}{\mathbf{q}^4} a^{00} + T^{\perp\perp}(\mathbf{q})\, a^{\perp\perp} \right\}. \tag{6}$$

We denote the angle between the electron and positron by θ and will use $x = \cos(\theta)$. Our dimensionless kinematic variable y is similar to that defined in Ref. [1], $\bar{E} - E' = yQ$, where Q is the total energy of the transition, and y can lie between $-(1 - \frac{2m_e}{Q})$ and $1 - \frac{2m_e}{Q}$; the difference in definitions is discussed below.[1] In Eq. (6), the kinematic functions a^{00} [5] and $a^{\perp\perp}$ are given by

$$a^{00} = \bar{E}E' + \bar{p}p'x - m_e^2 \tag{7}$$

and

$$a^{\perp\perp} = \bar{E}E' + m_e^2 - \frac{\mathbf{q}\cdot\bar{\mathbf{p}}\,\mathbf{q}\cdot\mathbf{p}'}{\mathbf{q}^2} = \bar{E}E' + m_e^2 - \frac{(\bar{p}^2 + \bar{p}p'x)(p'^2 + \bar{p}p'x)}{\mathbf{q}^2}. \tag{8}$$

We summarize in Table I the definition of the kinematic variables appearing in Eq. (8).

A. e^+e^- angular distributions for individual multipoles

The functions $T^{00}(\mathbf{q}^2)$ and $\mathrm{T}^{\perp\perp}(\mathbf{q}^2)$ are given above in terms of reduced nuclear matrix elements. We initially restrict our discussion to four electromagnetic multipoles, namely, scalar, vector, pseudoscalar, and tensor, or equivalently *C0, E1, M1,* and $E2$. We expand $T^{00}(\mathbf{q}^2)$ and $\mathrm{T}^{\perp\perp}(\mathbf{q}^2)$ in $\mathbf{q}^2$ and keep only leading-order terms. Using the definition of T^{00} in Eqs. (2) and (3) and expanding the Bessel functions $j_l(qx)$

[1] In Ref. [1] $\bar{E} - E' = yK$, where K is the sum of the lepton kinetic energies. This difference in definitions has no practical implications.

produce

$$T^{00} \cong \frac{\mathbf{q}^4 S}{36} + \frac{\mathbf{q}^2 D}{3} + \frac{\mathbf{q}^4 T}{225}. \tag{9}$$

The terms on the right-hand side of (9) determine the $C0$ (0^+), $E1$ (1^-), and $E2$ (2^+) transition rates via three nuclear-structure constants, S, D, and T, which are the squared reduced monopole, dipole, and quadrupole matrix elements, respectively.

The transverse-current structure function, $T^{\perp\perp}$, can be determined in a similar fashion. Expanding the spherical Bessel functions in Eq. (4) results in magnetic dipole (M), electric dipole (D), and electric quadrupole (T) contributions:

$$T^{\perp\perp} \cong \frac{2\mathbf{q}^2 M}{3} + \frac{2Q^2 D}{3} + \frac{\mathbf{q}^2 Q^2 T}{150}. \tag{10}$$

The structure constant M is the square of the reduced magnetic dipole matrix element. The proportionality of the O_{JM}^{J-1} and the C_{JM} for small q (viz., Siegert's theorem) was used to obtain the D and T terms. Of the four terms that remain (proportional to S, D, M, T), we keep the two (D and M) that have kinematic coefficients that are dimensionally equivalent to (energy)^2, and ignore the higher order terms, in common with other discussions. Note that in Eq. (6) magnetic multipoles occur only in $T^{\perp\perp}$, which then has the simple form given in Rose, but electric and Coulomb multipoles there are mixed between $T^{\perp\perp}$ and T^{00} in a most nonobvious (but correct) way.

B. Relation to the photon decay rate

The e^+e^- transition strength from the resonances of ^{8}Be to the ground state can be constrained by the corresponding photon transition strength, as was done by Rose [4], who calculated the leading-order e^+e^- decay rate "per photon." We have verified his results. In the case of γ decay with an outgoing photon of momentum $\mathbf{q}$ in the final state, the decay rate, ω_γ, is given by

$$\omega_\gamma = 2\alpha Q T^{\perp\perp}(-\mathbf{q}). \tag{11}$$

Thus the squared matrix elements M, D, and T entering the e^+e^- rates can, in principle, be extracted from measured γ-decay rates. Combining Eqs. (10) and (11) gives

$$\omega_\gamma \cong \frac{4\alpha}{3}\left(Q^3 M + Q^3 D + \frac{Q^5 T}{100}\right). \tag{12}$$

The squared $E0$ matrix element, S, must be determined by other means, if needed [5]. We will require only D and M, corresponding to electric dipole and magnetic dipole transitions.

III. ANALYSIS OF THE PHOTON DECAY DATA FOR ^{8}Be FROM THE ^{7}Li(p, γ) REACTION

The γ decays of the ^{8}Be resonances of interest have been measured via the analogous ^{7}Li(p, γ) reaction; the integrated cross section has been measured by Zahnow *et al.* [6] and the 90° excitation function by Fisher *et al.* [7]. The angular distributions for the emitted photons have been measured by Mainsbridge [8] and by Schlueter *et al.* [9]. The resonance

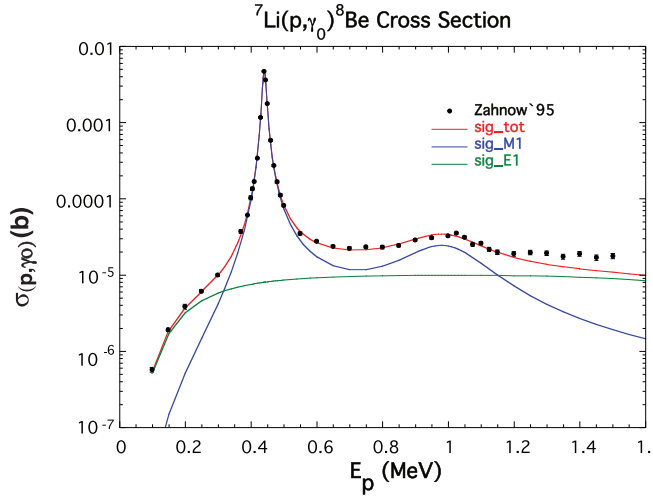

FIG. 1. The total integrated cross sections for the ^{7}Li$(p, \gamma)^8$Be reaction from Ref. [6]. The red curve is the result of our R-matrix fit to all of the available cross section and angular distribution data for the reaction. The blue and green curves show the $M1$ and $E1$ contributions to the cross section, respectively. The small peak centered at $E_p \approx 1$ MeV is the 18.15 MeV (1^+ $T = 0$) resonance, and the sharp peak at 0.4414 MeV is the 17.64 1^+ $T = 1$ resonance in ^{8}Be. From the R-matrix analysis, as well as from general arguments, the ratio of the magnetic to electric photon-decay strength varies strongly over the 18.15-MeV resonance.

energy range of interest is entirely dominated by $M1$ and $E1$ photon decay, and we used the measured cross sections and shape of the angular distributions in an R-matrix analysis to determine the magnitude of the $M1$ and $E1$ contributions to the cross section as a function of energy.

The R-matrix analysis contained two 1^+ ($M1$) levels, a very narrow one located at $E_x = 17.64$ MeV and a broader one at 18.15 MeV. In addition, there was a broad $E1$ (1^-) state located at $E_x = 22.0$ MeV that gives the tail of the giant dipole resonance, and fixed background poles located 10.63 MeV above and 3.0 MeV below the $p+^7$ Li threshold to mock up the effect of direct S-wave capture. All together, this gave 17 adjustable parameters to fit 279 data points, with χ^2 per degree of freedom of 3.18.

The R-matrix fit to the (p, γ) cross section data of Zahnow *et al.* is shown in Fig. 1. We find that over the resonance centered at 18.15 MeV ($E_p = 0.8$–1.2 MeV) the combination of $M1$ and $E1$ multipole strengths contributing to the (p, γ) reaction, and hence to the (p, e^+e^-) reaction, varies strongly with energy. This is because the $M1$ strength corresponds to a narrow (138 ± 6 keV) resonance centered at $E_x = 18.15$ ($E_p = 1.03$) MeV, whereas the $E1$ strength comes from the tail of the broad electric dipole structure centered close to $E_p = 5$ MeV. This $E1$ structure is evident in the data of Fisher *et al.*, Fig. 2. The prediction of a significant and broad direct s-wave $E1$ capture to the ^{7}Li(p, γ) and ^{7}Li(p, e^+e^-) reactions near $E_p = 5$ MeV is consistent with the analysis of Barker [10]. The ratio of $M1$ to $E1$ strength, together with its (shaded) 1-σ uncertainty, is shown in Fig. 3. That uncertainty was obtained by scaling the χ^2 from the R-matrix analysis to 1.0 while increasing error bars appropriately. Our analysis

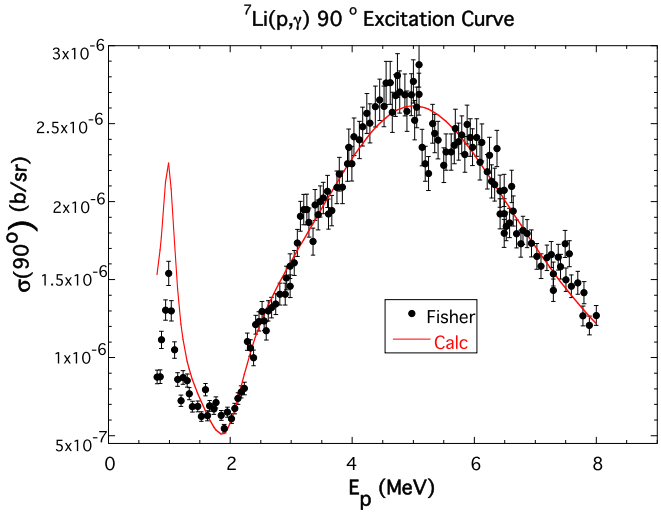

FIG. 2. The R-matrix fit to the 90° excitation function for the (p,γ) reaction. The data are from [7]. The R-matrix overestimate of the excitation function may reflect a theoretical $M1$ contribution that is too large, but it also reflects the fact that the Fisher [7] and Zahnow [6] measurements are not consistent with one another.

yields a very different energy dependence to the $M1/E1$ ratio than that assumed in Ref. [1], where a constant distribution of $M1 + 0.23E1$ was assumed over the energy region $E_p =$ 0.8–1.2 MeV. However, the large differences in widths of the $M1$ and $E1$ resonances rules out the possibility of the $M1/E1$ ratio being a constant. As discussed below, this strong energy-dependent variation in the $M1$ and $E1$ contributions to the (p,γ) and (p,e^+e^-) reactions has significant implications for any axion search close to the $E_p = 1.03$ MeV resonance in ^{8}Be.

The R-matrix analysis overestimates the 90° excitation function in the region of the 18.15-MeV resonance, which

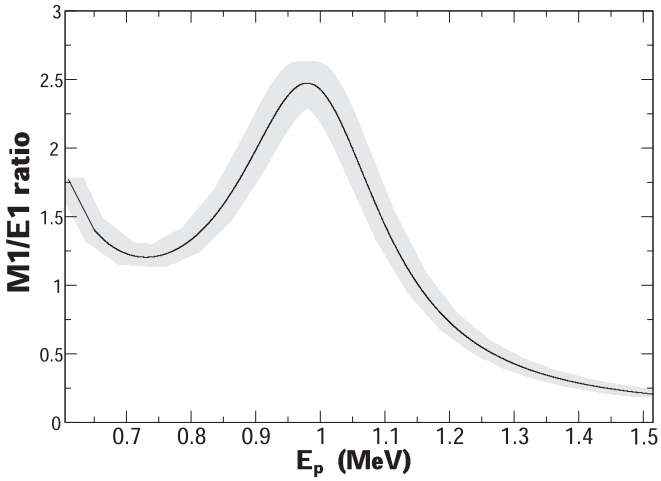

FIG. 3. The $M1$ to $E1$ photoabsorption cross section ratio from the R-matrix analysis of the (p,γ) cross section and angular distributions. At the peak of the $E_p = 1.03$ resonance, the cross section is approximately determined by an $M1 + 0.45E1$ combination, but above $E_p = 1.16$ MeV, the $E1$ contribution starts to dominate.

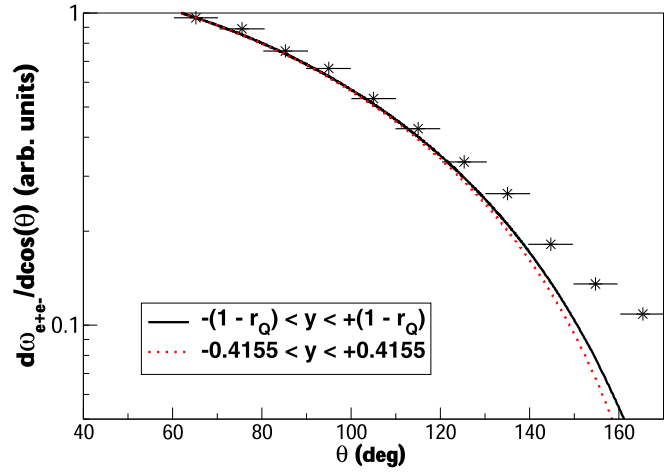

FIG. 4. The measured vs predicted angular distribution for the 6.05-MeV $0^+ \to 0^+$ $E0$ in ^{16}O. The straight line assumes no cuts on y and is in excellent agreement with the $E0$ angular distribution presented in Fig. 1 of Ref. [11]. The dotted line assumes cuts $-0.4155 < y < +0.4155$ $(-0.5 < y' < +0.5)$. In the limit that $m_e \to 0$ the $E0$ angular distribution is $1 + \cos(\theta)$, so that the slow falloff of the experimental angular distribution at large angles is difficult to understand.

may reflect an overestimate of the $M1$ strength in this region. However, the problem arises because the Zahnow and Fisher data sets are not consistent with one another at this energy. This can be understood by the following considerations: If the angular distributions are described by a Legendre polynomial expansion up through order $L = 2$, then the ratio of the 90° to the integrated cross section is determined by

$$R = \frac{4\pi\sigma(90^\circ)}{\sigma_{\rm int}} = 1 - \frac{1}{2}\frac{a_2}{a_0}, \tag{13}$$

in terms of the Legendre coefficients a_L. The maximum value of $\frac{a_2}{a_0}$ is obtained when only the transition $^3P_1(p+^7\text{Li}) \to$

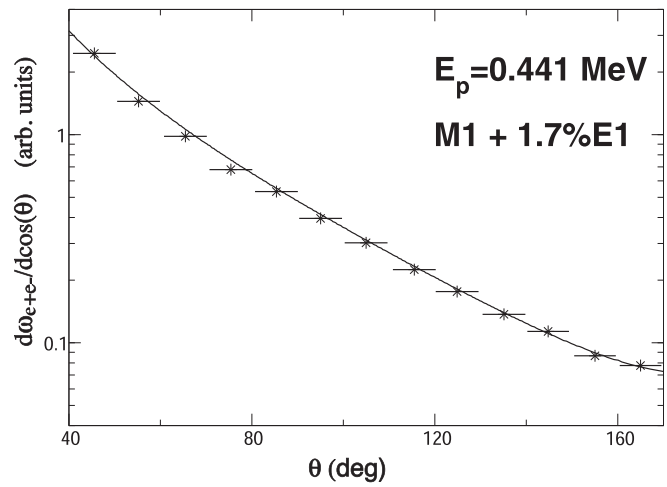

FIG. 5. The 1^+ transition at 17.64 MeV, which is predicted by our R-matrix analysis to be an $M1 + 1.7\%E1$ transition. This is in close agreement with the analysis of Ref. [1].

M1($\gamma + {}^8$ Be) is allowed, in which case the ratio has the value $\frac{1}{2}$. The presence of any other transition in the capture reaction, and in particular an $E1$ transition, dilutes this ratio so that $\frac{a_2}{a_0} < \frac{1}{2}$, meaning that the minimum value of R is 0.75. The value of R obtained from the R-matrix fit is 0.82 ± 0.029, reflecting the non-negligible amount of $E1$ cross section that contributes near the 1-MeV resonance (see Fig. 1). However, using the experimental values of the cross sections near 1 MeV from Fisher and Zahnow gives $R_{\rm exp} = 0.59 \pm 0.037$, which is well below the minimum possible value of R, and inconsistent with the calculated value within the uncertainties. Therefore, either the 90° cross section of Fisher is low, or the integrated cross section of Zahnow is high, at these energies. Given that Zahnow's measurement covers the range of both 1^+ (mostly) $M1$ resonances continuously, and it was done with five times better energy resolution than that of Fisher's, we tend to favor the explanation that the Fisher measurement is low in the peak of the 1-MeV resonance (see Fig. 2).

IV. THE ELECTRON-POSITRON ANGULAR DISTRIBUTIONS

The e^+e^- angular distribution can now be calculated by numerically integrating Eq. (6) with respect to the variable y. To be consistent with Ref. [1], we take the limits of integration to be $0.5 > y' > -0.5$, where $y' = (\bar{E} - E')/(\bar{k} + k')$, and $\bar{k}$ and k' are the kinetic energies of the positron and electron.

We find excellent agreement with the theoretical or simulated $0^+ \rightarrow 0^+$ $E0$ angular distribution presented in Fig. 1 of Ref. [11], if we assume a 6.05-MeV transition with no cuts on the observable y'. However, we do not reproduce the large angle portion of the ^{16}O 6.05 MeV in Fig. 2 of Ref. [1], if we assume that the cuts on y' are symmetric, as shown in Fig. 4. The experimental $E0$ angular distribution for this transition falls off slowly at large angles, with the ratio of the 65° to the 165° data points being slightly less than 10. In contrast, our predicted angular distribution falls off quite rapidly as $\theta \rightarrow 180°$, as shown in Fig. 4. The shape of the predicted $E0$ can

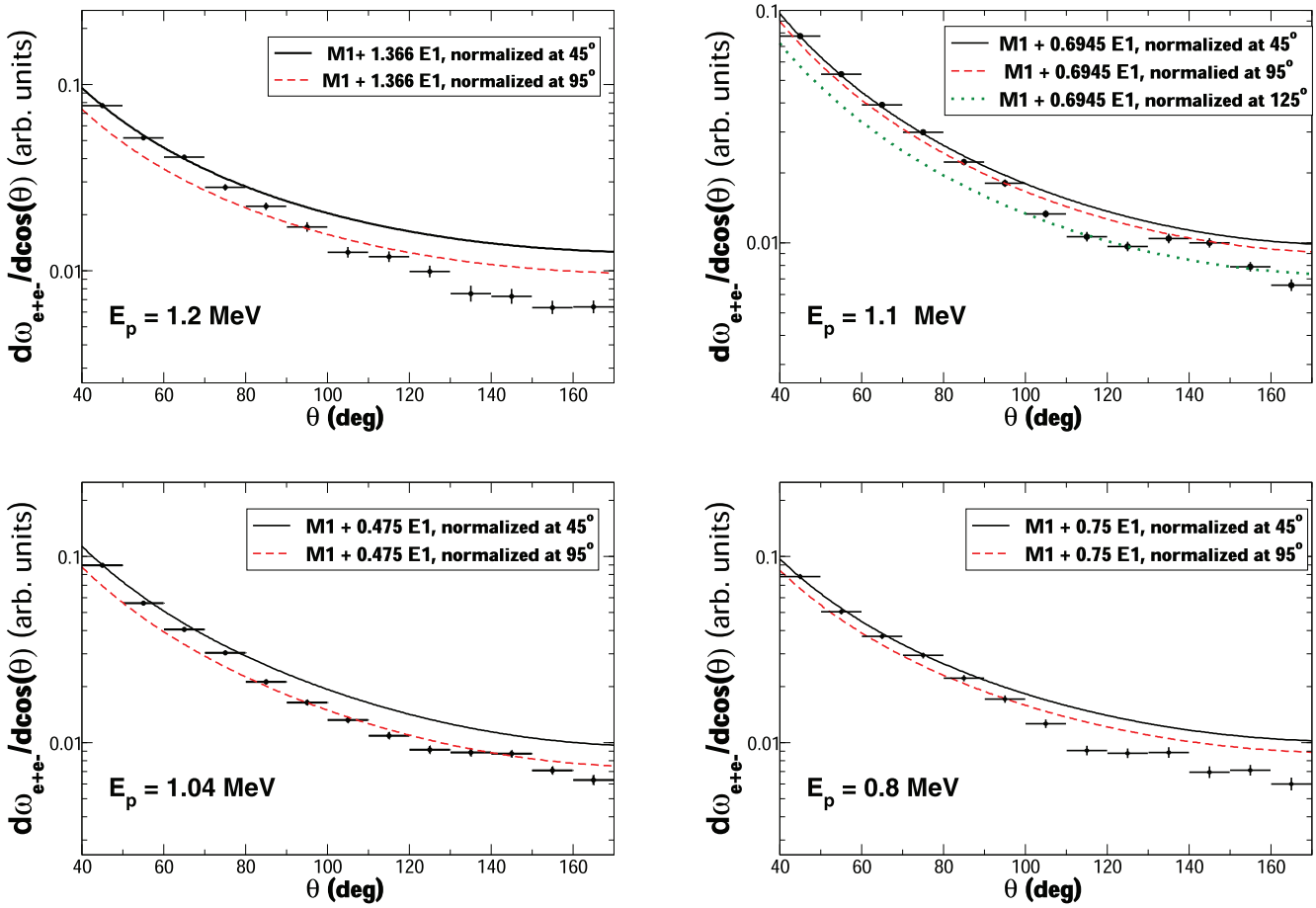

FIG. 6. The angular distributions for four proton beam energies that sweep across the 18.15-MeV resonance of ^{8}Be. At each energy, we take the relative $M1$ and $E1$ contribution to the angular distributions from our R-matrix analysis, as summarized in Fig. 3. If we normalize theory and experiment at forward angles, where the angular distribution is largest, we find the measured angular distributions are too low at backward angles. The theoretical angular distributions do not show any evidence of a bump and the bump seen in experiment lies below the expected angular distribution. In this sense, the experiment does not appear consistent with evidence for e^+e^- decay of a new particle. For the sake of displaying the bump more clearly, we also show the case where theory is normalized to experiment at 125° for $E_p = 1.1$ MeV, but this causes the comparison between theory and experiment at forward angles to be problematic.

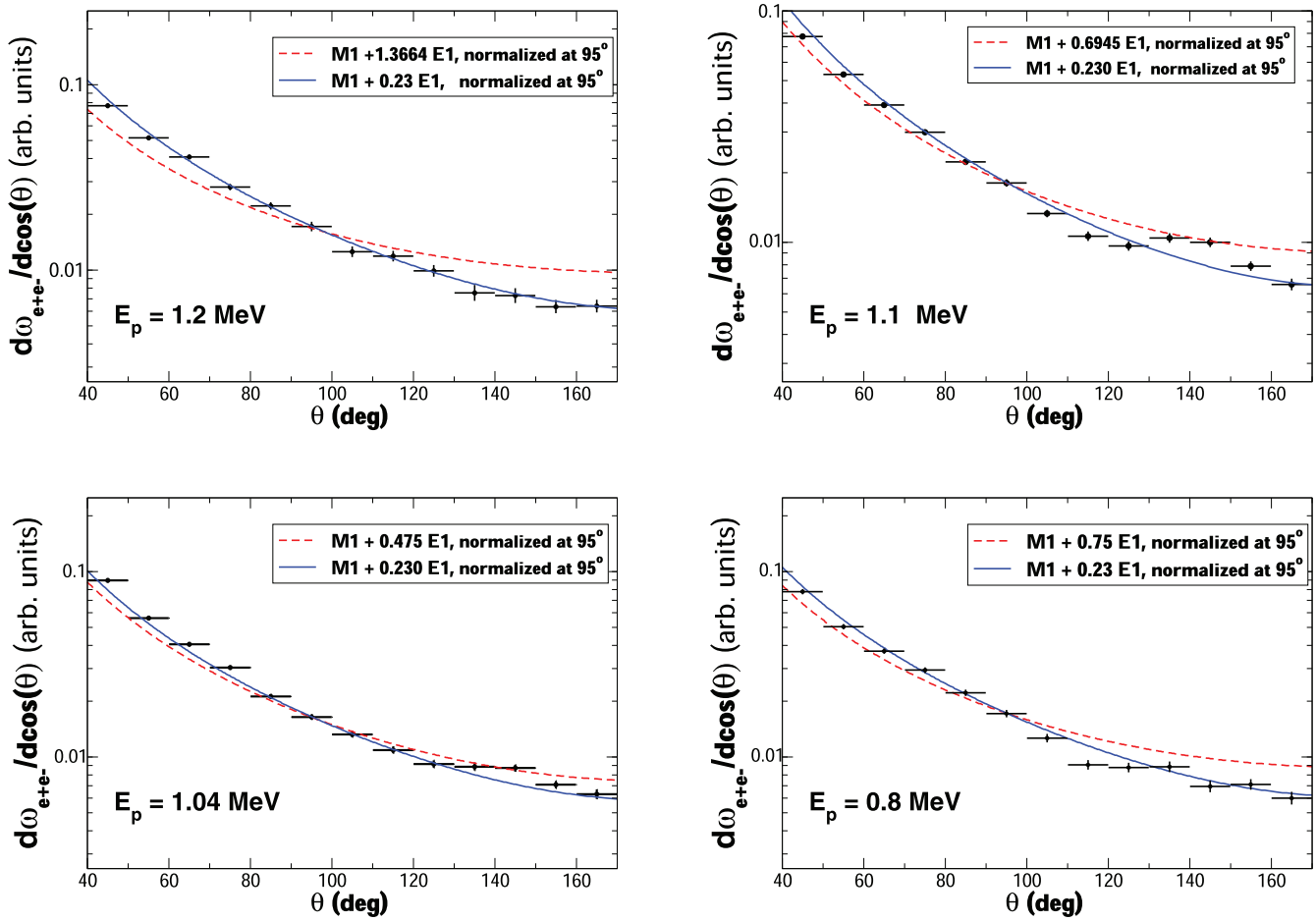

FIG. 7. The the same as Fig. 6, but with a comparison to the angular distribution assumed in Ref. [1], i.e., $M1 + 0.23E1$ (the blue curve). The experimental data do show a bump relative to the blue curve, but not relative to the expectations based on the (p, γ) reaction (the dashed red curve).

be understood by considering the limit in which $m_e \to 0$, in which case the $E0$ angular distribution is simply proportional to $1 + \cos(\theta)$, for any cuts on y'. When $m_e \neq 0$ and the cuts on y' are symmetric, the angular distribution falls off rapidly as one approaches 180°. A 65°/165° ratio close to 10 would only be possible if the cuts in y' were highly asymmetric.

We find good agreement with the measured [1] angular distribution for the 1^+ resonance in ^{8}Be excited by protons of energy $E_p = 0.441$ MeV for all measured angles, as shown in Fig. 5. Our R-matrix analysis predicts this resonance to correspond to an $M1 + 0.017E1$ transition, which is in close agreement to the analysis of Ref. [1]. However, we cannot reproduce the shape of the 1^+ resonance excited by proton energies between $E_p = 0.8$–1.2 MeV. The results for the latter resonance are shown in Fig. 6, where they are compared with the measured angular distributions of Ref. [1]. At each proton energy, the $M1/E1$ ratio is taken from our R-matrix analysis. We find that the measured angular distributions fall off faster that the theoretical predictions at large angles for proton energies between $E_p = 0.8$–1.2. This effect reflects the fact that the pure $M1$ angular distribution falls off more quickly at large angles that does the pure $E1$ angular distribution, and that the current analysis predicts considerably more $E1$ strength contributing to the resonance that that assumed in Ref. [1]. The highest $M1/E1$ ratio in the proton energy range 0.8–1.2 MeV region is found to be 2.5. As a result, the bumps observed in the experimental angular distributions fall below the standard model nuclear physics predictions. In this sense, the current analysis does not support the measured angular distribution being interpreted as evidence for the decay of a new axion particle.

Finally, in Fig. 7 we compare the measured angular distributions with the $M1/E1$ ratio assumed in Ref. [1], i.e., a constant ratio of $M1 + 0.23E1$. Under this assumption, the angular distributions at $E_p = 1.04$ and 1.1 MeV do show a bump above the expected angular distributions. Thus, we conclude that the evidence of a new axion particle being emitted from the 18.15-MeV resonance in ^{8}Be seems to be strongly dependent on the assumptions made about the nuclear structure of this resonance.

V. CONCLUSION

We have derived expressions for angular correlations for nuclear decay by e^+e^- decay, which are completely consistent with earlier expressions derived by Rose [4]. To establish

the appropriate combination of multipoles that apply in the region of the 18.15, 1^+ MeV resonance in ^{8}Be, we carried out an R-matrix analysis of the available cross sections and angular distributions for the ^{7}Li(p,γ) reaction. We find that the resonance region is entirely dominated by the $M1$ and $E1$ multipoles, but that the $M1$ to $E1$ ratio varies significantly with energy, being a maximum of $M1 + 0.455E1$ at the peak of the resonance ($E_p = 1.03$ MeV) and dropping to where $E1$ dominates over $M1$ above $E_p = 1.16$ MeV. This is in strong contrast to the assumptions of Ref. [1], that assumed a constant value of $M1 + 0.23E1$ over the range $E_p = 0.8$–1.2 MeV.

General arguments, which do not rely on the details of an R-matrix analysis, can be made to assert that the $M1/E1$ ratio cannot be constant over the 18.15, 1^+ MeV resonance, i.e., in the proton energy window $E_p = 0.8$–1.2 MeV. The $E1$ contribution in this energy window arises from the *very broad* and slowly varying tail of the giant dipole resonance, while the $M1$ strength is *very narrow* and rapidly varying in this window. Thus, there is no obvious physical mechanism to maintain a constant $M1/E1$ ratio. The minimum value for the $M1/E1$ ratio can also be argued on general, though less stringent, grounds. In particular, the giant dipole $E1$ resonance at ≈22 MeV above the ^{8}Be ground state has a broad measured [7] width of ≈5 MeV. This, combined with the narrow width of the 18.15-MeV $M1$ resonance, sets a lower limit on the $M1/E1$ ratio in the window $E_p = 0.8$–1.2 MeV. In the current work, we find the lower limit of the $M1/E1$ ratio to be about twice that assumed in the work of Ref. [1]. A ratio significantly lower than that found in the present work is not impossible, but it would require that the tail of the giant dipole fall off more quickly than expected as the proton energy is lowered below the peak of the $E1$ resonance. We are unaware of any nuclear structure arguments to support such a hypothesis.

The existence of a bump in the e^+e^- angular correlations at large opening angle is found to be strongly dependent on the assumptions made about the $M1/E1$ ratio in the energy interval associated with the $E_p = 1.03$ MeV 1^+ resonance. The current analysis indicates that the measured angular correlations fall off too rapidly with angle, falling below the R-matrix expectations at angles greater than 100°. In contrast, the nuclear structure assumptions made in the analysis applied in Ref. [1] would require the measured angular distributions at resonance to fall even more rapidly, creating the surplus events at large angles thus providing evidence for a new axion-like particle. At the least, a detailed remeasurement of the energy dependence of the $M1$ and $E1$ yields in the (p,γ) reaction in this energy range would be needed before the unexpected observation of a non-standard model particle should be claimed.

[1] A. J. Krasznahorkay, M. Csatlos, L. Csige, Z. Gacsi, J. Gulyas, M. Hunyadi, I. Kuti, B. M. Nyako, L. Stuhl, J. Timar, T. G. Tornyi, Zs. Vajta, T. J. Ketel, and A. Krasznahorkay, Phys. Rev. Lett. **116**, 042501 (2016).

[2] X. Zhang and G. A. Miller, Phys. Lett. B **773**, 159 (2017).

[3] X. Zhang and G. A. Miller, Phys. Lett. B **813**, 136061 (2021).

[4] M. E. Rose, Phys. Rev. **76**, 678 (1949). This paper separately calculates $\frac{d^2\omega_{e^+e^-}}{dxdy}/\omega_\gamma$ for each electric and magnetic multipole in the limit of small q, and the nuclear matrix element cancels in the ratio. Note that his energies are all divided by the electron rest energy.

[5] J. L. Friar, Ann. Phys. (NY) **95**, 170 (1975).

[6] D. Zahnow, C. Angulo, C. Rolfs, S. Schmidt, W. H. Schult, and E. Somorjai, Z. Phys. A **351**, 229 (1995).

[7] G. A. Fisher, P. Paul, F. Riess, and S. S. Hanna, Phys. Rev. C **14**, 28 (1976).

[8] B. Mainsbridge, Nucl. Phys. **21**, 1 (1960).

[9] D. J. Schlueter, R. W. Krone, and F. W. Prosser, Nucl. Phys. **58**, 254 (1964).

[10] F. C. Barker, Aust. J. Phys. **49**, 1081 (1996).

[11] J. Gulyás, T. J. Ketel, A. J. Krasznahorkay, M. Csatlós, L. Csige, Z. Gácsi, M. Hunyadi, A. Krasznahorkay, A. Vitéz, and T. G. Tornyi, Nucl. Inst. Meth. Phys. Res. A **808**, 21 (2016).